Please cite the Published Version

Additional Information: This is an open access article which first appeared in Journal of Cellular Physiology, published by Wiley

Data Access Statement: The data that support the findings of this study are available from the corresponding author upon reasonable request.

RESEARCH ARTICLE

A combination of major histocompatibility complex (MHC) I overexpression and type I interferon induce mitochondrial dysfunction in human skeletal myoblasts

Anastasia Thoma[1] | Razan Alomosh[1] | Holly L. Bond[1] | Tania Akter-Miah[1] |
Nasser Al-Shanti[1] ⦿ | Hans Degens[1,2] | Vanja Pekovic-Vaughan[3] |
Adam P. Lightfoot[1] ⦿

[1]Department of Life Sciences, Faculty of Science & Engineering, Manchester Metropolitan University, Manchester, UK

[2]Institute of Sport Science and Innovations, Lithuanian Sports University, Kaunas, Lithuania

[3]Department of Musculoskeletal and Ageing Science, Faculty of Health and Life Science, University of Liverpool, Liverpool, UK

Correspondence
Adam P. Lightfoot and Anastasia Thoma
Email: a.lightfoot@mmu.ac.uk and natasa.thoma@gmail.com

Abstract

The overexpression of major histocompatibility complex (MHC) I on the surface of muscle fibers is a characteristic hallmark of the idiopathic inflammatory myopathies (IIMs), collectively termed myositis. Alongside MHC-I overexpression, subtypes of myositis, display a distinct type I interferon (IFN) signature. This study examined the combinational effects of elevated MHC-I and type I IFNs (IFNα/β) on mitochondrial function, as mitochondrial dysfunction is often seen in IIMs. Human skeletal muscle myoblasts were transfected with an MHC-I isoform using the mammalian HLA-A2/K^b vector. Mitochondrial respiration, mitochondrial membrane potential, and reactive oxygen/nitrogen species generation were assessed with or without IFNα and IFNβ. We show that MHC-I overexpression in human skeletal muscle myoblasts led to decreased basal glycolysis and mitochondrial respiration, cellular spare respiratory capacity, adenosine triphosphate-linked respiration, and an increased proton leak, which were all exaggerated by type I IFNs. Mitochondrial membrane depolarization was induced by MHC-I overexpression both in absence and presence of type I IFNs. Human myoblasts overexpressing MHC-I showed elevated nitric oxide generation that was abolished when combined with IFN. MHC-I on its own did not result in an increased reactive oxygen species (ROS) production, but IFN on their own, or combined with MHC-I overexpression did induce elevated ROS generation. Surprisingly, we observed no gross changes in mitochondrial reticular structure or markers of mitochondrial dynamics. We present new evidence that MHC-I overexpression and type I IFNs aggravate the effects each has on mitochondrial function in human skeletal muscle cells, providing novel insights into their mechanisms of action and suggesting important implications in the further study of myositis pathogenesis.

KEYWORDS
idiopathic inflammatory myopathies, major histocompatibility complex I, mitochondria, myositis, reactive and nitric oxygen species, type I interferon

1 | INTRODUCTION

The idiopathic inflammatory myopathies (IIMs) are a group of rare acquired inflammatory muscle diseases, collectively known as myositis. Patients with myositis share some common clinical features, including muscle weakness, increased circulating muscle enzymes (e.g., creatine kinase), inflammatory infiltration of CD4$^+$/CD8$^+$ T-cells and B-cells within the muscle, expression of muscle-specific and -associated autoantibodies and interferon (IFN) upregulation in muscle fibers, and overexpression of major histocompatibility complex class I (MHC-I) on the surface of muscle fibers (Carstens & Schmidt, 2014).

A recent study demonstrated that IFN signature facilitates stratification of IIMs, where, for instance, elevated expression of both type I IFNα and IFNβ is unique to dermatomyositis (Rigolet et al., 2019). The significance of type I IFN is illustrated by the fact that IFN-I treatment of human peripheral blood mononuclear cells and skeletal muscle cells induced a gene expression profile that was largely identical to that observed in patients with dermatomyositis (Arshanapalli et al., 2015). IFN-inducible genes were also present in blood samples of patients with dermatomyositis and polymyositis and correlated with disease type. Specifically, dermatomyositis samples presented higher levels of type I IFN-inducible genes compared to polymyositis, while none were found in inclusion body myositis (Walsh et al., 2007). The distinct type I IFN signature in dermatomyositis as well as the overexpression of MHC-I have turned the attention to their role in downstream pathology-associated mechanisms. Sustained upregulation of MHC-I in muscle has displayed a positive correlation with endoplasmic reticulum stress activation (Fréret et al., 2013; Thoma et al., 2022), which has been evident in patients with myositis (Nagaraju et al., 2005). Perifascicular atrophy is a histological hallmark of dermatomyositis, and studies have shown that mitochondrial abnormalities and MHC I overexpression, are predominantly localized to these fibers undergoing atrophy (Alhatou et al., 2004).

A recent study highlighted the involvement of mitochondrial damage, by the mitochondria-localized proapoptotic hara-kiri protein, in myofiber death and muscle weakness in individuals with dermatomyositis and polymyositis (Boehler et al., 2019). A further study showed decreased expression of genes associated with mitochondrial biogenesis and those encoding proteins of the electron transport chain complexes in muscle fibers from a dermatomyositis patient and in a murine experimental autoimmune model of myositis (Meyer et al., 2017). This study also demonstrated reduced mitochondrial respiration and increased reactive oxygen species (ROS) generation in each model. Furthermore, they provided evidence that the type I IFN score correlated with mitochondrial respiratory deficiency in dermatomyositis muscle, while IFN-β treatment of human myotubes decreased mitochondrial respiration in a ROS-dependent manner (Meyer et al., 2017).

Both type I IFN signature and MHC-I have been suggested to play an important role in dermatomyositis and polymyositis. Despite the evidence of mitochondrial abnormalities in myositis, to our knowledge, the role of sustained MHC-I upregulation on mitochondrial function (Danieli et al., 2023) remains to be revealed. Likewise, little is known about the distinct effects of IFNα and IFNβ on mitochondrial function. Therefore, we have generated an in vitro MHC-I human skeletal muscle model that overexpresses human leukocyte antigen (HLA) class I (the so-called MHC-I system in humans) (Cruz-Tapias et al., 2013). Using this model, the present study brings insights not only into the role of MHC-I overexpression on mitochondrial function in human muscle cells, but also presents the distinct effects of type I IFNα/β in the presence or absence of MHC-I overexpression. Our data reveals for the first time that MHC-I overexpression in human muscle cells acts synergistically with type I IFNs resulting in mitochondrial respiratory defects and that each on their own present distinct effects on reactive oxygen and nitrogen species production.

2 | MATERIALS AND METHODS

2.1 | Cell culture

An immortalized human skeletal muscle cell line was a gift from the Center for Research in Myology in Paris (France) (Mamchaoui et al., 2011). Cells were grown under standard cell culture conditions (37°C, 5% CO_2) in growth media (GM) containing: Dulbecco's Modified Eagles Medium, high-glucose (4.5 g/L DMEM) and Medium-199 with Earle's BSS (1:5, v/v) (Sigma-Aldrich), 20% (v/v) heat-inactivated fetal bovine serum (Gibco), 1% (v/v) penicillin/streptomycin, 1% (v/v) L-glutamine (Lonza), 10 µg/mL gentamicin, 25 ng/mL fetuin from fetal bovine serum, 0.2 µg/mL dexamethasone, 5 µg/mL recombinant human insulin (Sigma-Aldrich), 0.5 ng/mL recombinant human basic fibroblast growth factor, 5 ng/mL recombinant human epidermal growth factor, and 2.5 ng/mL recombinant human hepatocyte growth factor (Gibco).

2.2 | Plasmid preparation

Psv2-neo plasmid containing HLA-A2/K^b was a gift from Linda Sherman (Addgene #14906) (Irwin et al., 1989). Psv2-neo empty vector (EV) plasmid in *Escherichia coli* was purchased from ATCC (#37149). The plasmid DNA (pDNA) was amplified by creating single colonies of *E. coli* in agar plates and incubated in Lennox L Broth (LB Broth; Invitrogen). The pDNA was stored as glycerol stocks and purified using QIAprep spin miniprep kit (Qiagen). The concentration was determined before use and only pDNA with 260/280 > 1.80 and 260/230 > 2.0 was used.

2.3 | Transfection and treatments

Human skeletal muscle myoblasts were seeded 24 h before transfection to achieve 70%–90% confluence. At the time of transfection, the GM was replaced with fresh GM. Cells were incubated with the

transIT-X2 (Mirus): plasmid (EV or HLA-A2/K^b; 1 μg/μL) complex at 2:1 ratio prepared in Opti-MEM (Gibco) for 18 h in the presence or absence of 100 ng/mL type I IFNα (PBL Assay Science) or IFNβ (R&D Systems).

2.4 | Assessment of transfection efficiency by immunostaining

Transfection efficiency was determined by immunostaining. Human skeletal muscle myoblasts were fixed in 4% paraformaldehyde (Alfa Aesar) (15 min, room temperature) and permeabilised using 0.5% Triton X-100 (Sigma) (15 min, room temperature). Cells washed in Dulbecco's Phosphate-Buffered Saline (DPBS, Lonza) were blocked using 3% goat serum (Vector Laboratories) in 0.05% Tween-20 (Fisher Scientific) in PBS for 1 h at room temperature. Washed cells were incubated with anti-HLA class I antibody (1/1000, Abcam #ab23755) at 4$^°$C overnight and stained with goat antimouse IgG (H + L) Alexa Fluor 488 (1/800, Invitrogen) and 4′,6′-diamidino-2-phenylindole dihydrochloride (DAPI, 1/3000, Sigma-Aldrich) for 1 h at room temperature protected from ambient light. Cells maintained in DPBS were imaged using a LEICA DMI6000 B inverted microscope (CTR6000 laser, Leica Microsystems).

2.5 | Assessment of cellular respiration using seahorse extracellular flux analysis

Mitochondrial function and glycolytic activity were measured with an XFp Extracellular Flux Analyser (Agilent Technologies). Human skeletal muscle cells were seeded in an 8-well XFp plate at a density of 7 × 10^3 cells/well in GM. After overnight incubation, cells were transfected with the HLA-A2/K^b overexpression vector or EV in the presence or absence of type I IFNα or IFNβ, as described above. Real-time oxygen consumption rate (OCR) and extracellular acidification rate (ECAR), as a measure of mitochondrial respiration and basal glycolysis, respectively (Dott et al., 2014), were assessed using the Seahorse XFp Mito Stress Test (Agilent Technologies). GM was replaced with Seahorse assay medium containing unbuffered DMEM (pH 7.4), 1 mM pyruvate (Agilent Technologies), 2 mM L-glutamine, and 10 mM glucose (Agilent Technologies), and myoblasts were incubated at 37°C in a non-CO$_2$ incubator 1 h prior the experiment. The sequential addition of oligomycin (1 μM), carbonyl cyanide-p-trifluoromethoxyphenylhydrazone (FCCP) (2 μM), and rotenone/antimycin (0.5 μM) enabled the analysis of the cell bioenergetic phenotype parameters. Oligomycin, an adenosine triphosphate (ATP) synthase inhibitor, was injected to enable measurement of ATP-linked respiration. This also allowed assessment of proton leak, as the basal respiration that is not used for ATP production. The uncoupling agent FCCP was added to disrupt OCR and ECAR, normalized to total protein concentration using the Pierce™ BCA Protein Assay (Thermo Scientific), calculated by Seahorse XFp Wave software version 2.2.0 (Agilent Technologies).

2.6 | Assessment of mitochondrial membrane potential and mass

Human skeletal muscle myoblasts were seeded at 8 × 10^3 cells/well in a black-sided, clear-bottom microplate (96 wells), cultured in GM, and transfected and treated as described above. JC-1 fluorophore (5,5′,6,6′-tetrachloro-1,1′,3,3′-tetraethylbenzimi-dazolylcarbocyanine iodide) (Abcam), MitoTracker Red CMXRos and TMRM (Tetramethyl-lrhodamine, methyl ester) (Molecular Probes, Invitrogen, Paisley) were used to assess mitochondrial membrane potential (ΔΨm). Human skeletal muscle myoblasts were incubated with JC-1 (5 μM, 30 min, 37°C) in the presence of transfection solution (HLA-A2/K^b or EV) with or without type I IFNs, in the dark. Following incubation with JC-1, cells were washed with DPBS and maintained in GM-containing type I IFN treatments, and fluorescence intensities from JC-1 aggregate and monomer forms were measured at excitation 530/25 and 485/20 nm, respectively, and emission 590/35 nm. Changes in TMRM fluorescence intensity were normalized to mitochondrial mass by washing myoblasts transfected with HLA-A2/K^b or EV with or without type I IFNs with warm DPBS and incubating them with TMRM/MitoTracker Green FM (Invitrogen) (10 and 100 nM, respectively, 30 min, 37°C). Fluorescence intensity was read in the presence of staining solution at 530/25 nm excitation and 590/35 nm emission for TMRM and 485/20 nm excitation and 528/20 nm emission for MitoTracker Green FM. To assess MitoTracker Red CMXRos fluorescence intensity, myoblasts were washed with warm DPBS and stained in 5 μM MitoTracker Red CMXRos solution (30 min, 37°C) and fluorescence was measured in cells maintained in phenol red-free DMEM at excitation 590/20 and emission 645/40 nm. Endpoint fluorescence for all probes was measured using a SynergyTM multidetection microplate reader (BioTek Instruments). All measurements were corrected for background fluorescence and normalized to total protein content.

2.7 | Measurement of reactive oxygen/nitrogen species

To quantify mitochondrial superoxide and hydroxyl radical generation, human myoblasts transfected with HLA-A2/K^b or EV +/- type I IFNs were seeded in a black-sided, clear-bottom microplates (96 wells), washed with DPBS and incubated with either a MitoSOX™ Red mitochondrial superoxide indicator (5 μM, 30 min, 37°C) (Invitrogen) or OH580 probe, a mitochondrial hydroxyl radical indicator (1 h, 37°C) (Abcam) in phenol red-free DMEM in the dark. Following incubation, cells were washed with DPBS, maintained in assay medium, and endpoint fluorescence was measured with the following excitation and emission wavelengths: MitoSOX™ Red, 360/40 and 590/35 nm; and OH580 probe, 530/25 and 590/35 nm, respectively. To assess intracellular nitric oxide generation, 4-amino-5-methylamino-2',7'-difluorofluorescein diacetate (DAF-FM-DA) (10 μM) (Abcam) was added to the cells in the presence of transfection solution ± type I IFNs. Following 30 min incubation at 37°C,

cells were washed with DPBS, maintained in GM ± type I IFNs, and endpoint fluorescence was measured at 485/20 nm excitation and 528/20 nm emission. Amplex® Red Hydrogen Peroxide/Peroxidase assay (Invitrogen) was used to measure hydrogen peroxide (H_2O_2) released from cells according to the manufacturer's instructions. Briefly, cell culture media and standard curve samples of known H_2O_2 concentrations were incubated with the Amplex® Red reagent (100 μM)/Horseradish peroxidase (0.2 U/mL) solution at room temperature for 30 min and endpoint fluorescence was measured at 530/25 nm excitation and 590/35 nm emission. Endpoint fluorescence for all probes was measured using a Synergy™ multidetection microplate reader (BioTek Instruments). All measurements were corrected for background fluorescence and normalized to total protein content.

2.8 | Mitochondrial imaging

Mitotracker red staining was conducted as we have previously described (Thoma et al., 2020). Briefly, human skeletal myoblasts were cultured on Matrigel-coated 35 mm dishes and transfected with HLA-A2/K[b] or EV in presence or absence of type I IFNs. Cells were loaded with MitoTracker Red CMXRos(5 μM, 30 min, 37∘C) (Molecular Probes, Invitrogen) selective for living mitochondria, and fixed in 4% paraformaldehyde. Nuclei were counter-stained with DAPI (1/5000) (Sigma-Aldrich, Dorset). Cells were imaged on a Leica Stellaris 5, confocal system. Mitochondrial network analysis was undertaken using the MiNA plugin for Fiji (Valente et al., 2017).

2.9 | Quantitative polymerase chain reaction (qPCR)

RNA was isolated using a Total RNA extraction kit (Norgen), and cDNA synthesized using Bio-Rad iScript first-strand kit. qPCR was conducted as previously described (Thoma et al., 2020). Primer sequences can be found in Table 1, data were normalized to 18S housekeeping gene, in accordance with the delta-delta-ct method.

2.10 | Statistical analyses

Statistical analyses were performed with GraphPad Prism version 8. Data were assessed for normality of distribution using Shapiro–Wilk test. Normally distributed data were analyzed using one-way analysis of variance followed, where appropriate, by Tukey's post hoc test, and nonnormally distributed data using Kruskal–Wallis test with Dunn's post hoc test. A $p ≤ 0.05$ was considered statistically significant.

3 | RESULTS

3.1 | IFNα and IFNβ present a differential impact on mitochondrial respiration

We initially examined the effects of the type of IFNs on the mitochondrial function of human skeletal muscle cells using Seahorse Extracellular Flux Analyser. 18 h exposure to 100 or 200 ng/mL IFNα treatment did not induce any significant changes in mitochondrial function parameters, including spare respiratory capacity, basal, maximal, ATP-linked, and leak respiration, nor did it affect nonmitochondrial respiration (Figure 1a–f). Mitochondrial bioenergetics remained unaffected following 24 h treatment with 100 ng/mL IFNα, while higher IFNα concentration (200 ng/mL) significantly reduced oxygen consumed for basal and ATP-linked respiration only, indicating the initiation of mild effects on mitochondrial function by a longer exposure of human muscle cells to IFNα (Figure 1g–l).

In contrast to IFNα treatment, treatment of human myoblasts with 100 or 200 ng/mL of IFNβ for 18 h induced a significant reduction in basal, maximal, and ATP-linked respiration, while defects in nonmitochondrial respiration were induced by 200 ng/mL IFNβ only (Figure 2b–f). It should be noted that 18 h exposure to IFNβ at either concentration did not induce changes in spare respiratory capacity or leak respiration (Figure 2d,e). Interestingly, lower proton leak was seen following 24 h treatment with IFNβ (Figure 2k), with no discernable changes being evident in other mitochondrial function parameters (Figure 2g–l).

TABLE 1 List of human primers used in the qPCR experiments.

Gene	Forward primer	Reverse primer
18S	CGGCTACCACATCCAAGGAAGG	CCCGCTCCCAAGATCCAACTAC
MFN1	AGTTGGAGCGGAGACTTAGC	ATCGCCTTCTTAGCCAGCAC
MFN2	TGACGCGCTTATCCACTTCC	CATTGCGCTTCACCTTCCC
PPARGC1A	TGACTGGCGTCATTCAGGAG	AACCAGAGCAGCACACTCG
FIS1	AGGCCTTAAAGTACGTCCGC	TGCCCACGAGTCCATCTTTC
TFAM	GAACAGCTAACTCCAAGTCAGA	CAGCTTTTCCTGCGGTGA
DRP1	TCACCCGGAGACCTCTCATT	TCTGCTTCCACCCCATTTTCT

Abbreviation: qPCR, quantitative polymerase chain reaction.
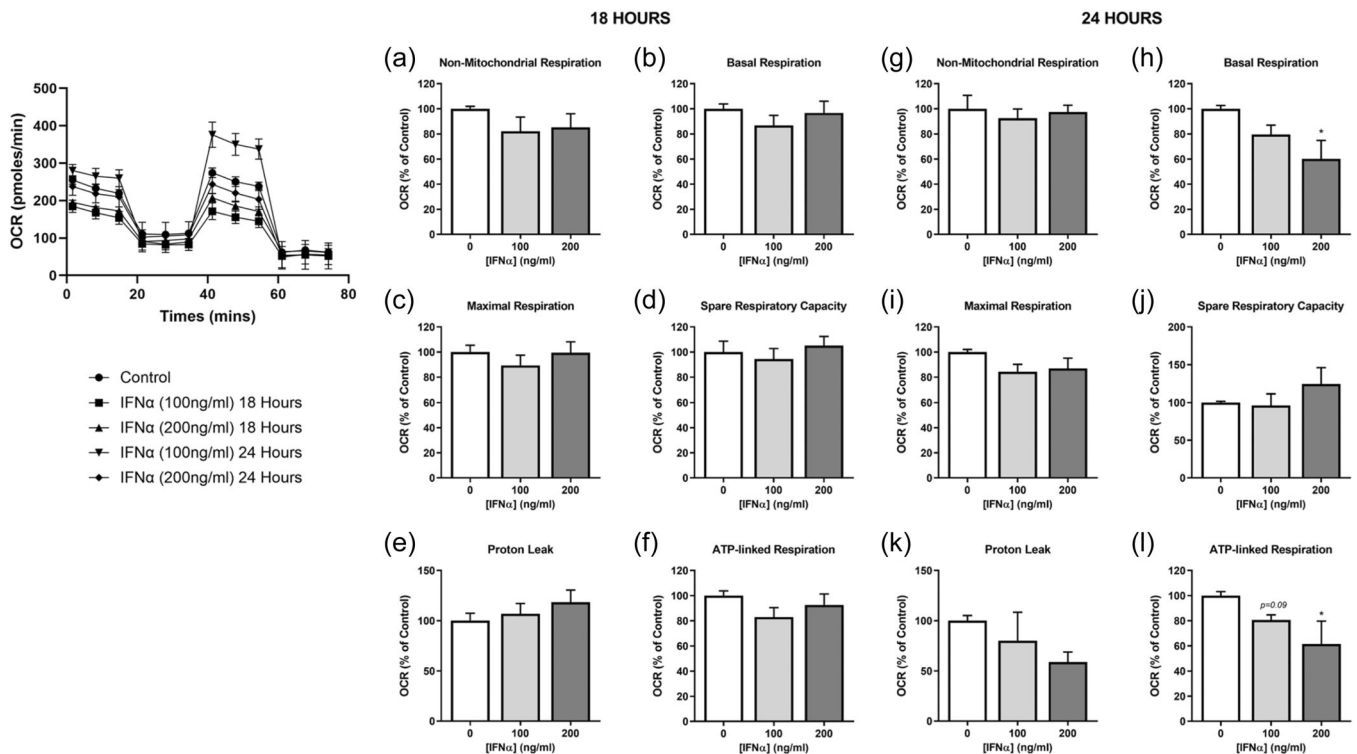
FIGURE 1 Mitochondrial function of human myoblasts treated with interferon-α (IFNα). Non-mitochondrial respiration, basal respiration, maximal respiration, spare respiratory capacity, proton leak, and ATP-linked respiration, normalized to protein content following 18 h (a–f) and 24 h (g–l) incubation with IFNα at indicated doses ($n = 6$). Data represent mean ± SEM, $^*p \leq 0.05$ compared to control. ATP, adenosine triphosphate; SEM, standard error of the mean.

3.2 | MHC-I levels following transfection with HLA-A2/K^b vector in the presence or absence of type I IFNs

We next transfected human skeletal cells with either EV or HLA-A2/K^b vectors and examined their expression using fluorescence microscopy. Transfection of human skeletal myoblasts with the HLA-A2/K^b vector resulted in significantly upregulated MHC-I expression compared to EV as shown by changes in fluorescence intensity levels of HLA (green channel fluorescence) normalized to nuclei number (blue channel fluorescence) (Figure 3). Interestingly, IFNα exposure of MHC-I overexpressing human myoblasts induced significantly higher HLA fluorescence intensity levels (by 78.2%), compared to HLA-transfected myoblasts alone. In contrast, IFNβ exposure of MHC-I overexpressing human myoblasts increased HLA fluorescence intensity only by 20.5%, compared to MHC-I expression alone (Figure 3a,b).

## 3.3 | MHC-I overexpression-induced changes in cellular metabolism are exacerbated by type I IFNs

Overexpression of MHC-I in human skeletal muscle myoblasts induced a reduction in both mitochondrial respiration (OCR) and basal glycolysis (ECAR) as assessed by Seahorse Extracellular Flux

Analyser, which was exacerbated in the presence of 100 ng/mL type I IFNs (IFNα or IFNβ) following 18 h exposure (Figure 4a–d). MHC-I overexpressing myoblasts in the presence of IFNβ also showed a significantly reduced nonmitochondrial respiration (Figure 4e). Mitochondrial OCR was suppressed at both basal and maximal capacities by MHC-I overexpression, which was exacerbated in the presence of IFNα or IFNβ, with IFNβ showing stronger effects (Figure 4f,g). Decreased mitochondrial respiration was accompanied by significantly decreased ATP-linked respiration in MHC-I overexpressing human myoblasts, with IFNβ inducing the largest decrease, followed by IFNα, when compared to EV (Figure 4i). IFNβ treatment of MHC-I overexpressing myoblasts also significantly decreased spare respiratory capacity (Figure 4h). Moreover, proton leak respiration was decreased by MHC-I overexpression, with combinatorial IFNα or IFNβ treatments leading to a higher rate of change, when compared to EV (Figure 4j).

3.4 | MHC-I overexpression in the presence of type I IFNs induces changes in mitochondrial mass and membrane potential

Different fluorophores were used as probes to assess changes in mitochondrial membrane potential in response to MHC-I
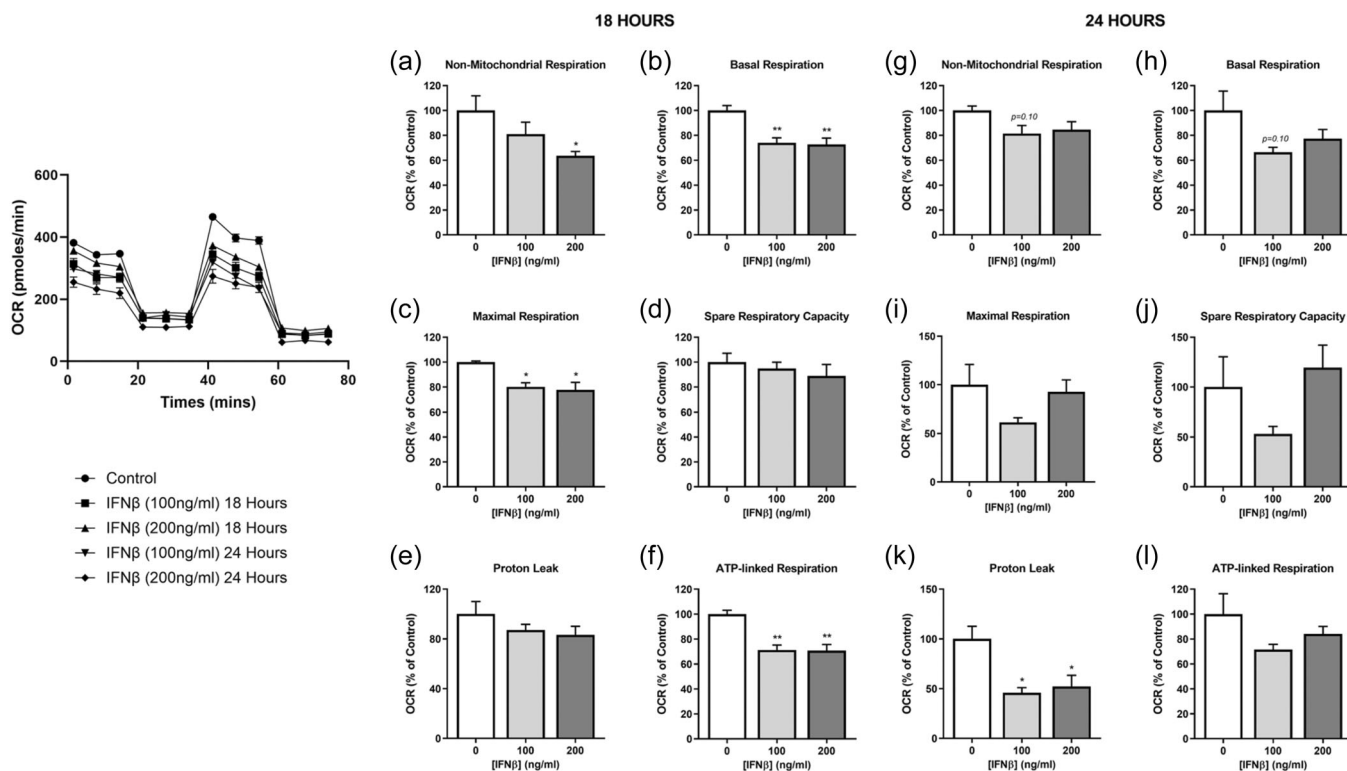
FIGURE 2 Mitochondrial function of human myoblasts treated with interferon-β (IFNβ). Non-mitochondrial respiration, basal respiration, maximal respiration, spare respiratory capacity, proton leak, and ATP-linked respiration, normalized to protein content following 18 h (a–f) and 24 h (g–l) incubation with IFNβ at indicated doses (*n* = 6). Data represent mean ± SEM, *$p ≤ 0.05$, **$p < 0.01$ compared to control. ATP, adenosine triphosphate; SEM, standard error of the mean.

overexpression of human myoblasts in the presence or absence of type I IFNs. We first determined the mitochondrial membrane potential using the ratiometric dye JC-1, which reflects the ratio of JC1-aggregates formed in active (negatively charged) mitochondria versus JC1-monomers present in depolarized mitochondria (Sivandzade et al., 2019). The JC-1 ratio was significantly decreased in MHC-I overexpressing human muscle cells, with type I IFNs inducing a higher rate of decrease by approximately 35% compared to MHC-I overexpressing cells alone (Figure 5a). We also utilized another mitochondria-based dye, TMRM, which accumulates solely in active mitochondria with intact membrane potential. MHC-I overexpression in combination with IFNα, but not IFNβ, induced a significant increase in TMRM fluorescence (Figure 5c). MHC-I overexpression in combination with IFN, but not on its own, induced a significant increase in mitochondrial mass as assessed by MitoTracker Green FM fluorescence intensity (Figure 5d). However, when the TMRM fluorescence signals were normalized to mitochondrial mass using MitoTracker Green FM, the TMRM fluorescence intensity was reduced, rather than increased in MHC-I overexpressing cells in the presence of IFNβ treatment (Figure 5e). The MitoTracker Red CMXROS probe, which accumulates in active mitochondria, showed no significant change in fluorescence intensity in MHC-I myoblasts both in the absence and presence of type I IFNs (Figure 5b).

3.5 | MHC-I overexpression in human myoblasts leads to increased nitric oxide generation, while mitochondrial superoxide is elevated in the presence of combined treatment with IFNβ

We then examined reactive oxygen & nitrogen species (RONS) production in MHC-I overexpressing human myoblasts in the absence or presence of type I IFNs. Type I IFNs alone led to a significant increase in mitochondrial superoxide production as assessed by MitoSOX Red compared to control myoblasts (Figure 6a), while MHC-I overexpressing cells did not show an elevated ROS production (Figure 6b). An increase in MitoSOX Red fluorescence intensity in MHC-I-overexpressing myoblasts was only observed in the presence of type I IFNβ (Figure 6b), while no significant change was observed in the case of IFNα treatment (Figure 6b).

Overexpression of MHC-I alone promoted an increased intracellular nitric oxide (NO) generation in human myoblasts compared to the EV-expressing myoblasts, indicated by the increased DAF-FM DA fluorescence intensity (Figure 6c). The NO levels were also substantially higher in MHC-I overexpression alone compared to MHC-I overexpression + IFNβ treatment (Figure 6c). Lastly, there was no change in H_2O_2 release from human myoblasts as assessed by Amplex Red following MHC-I overexpression in the absence or presence of type I IFNs compared to EV-expressing myoblasts (Figure 6d).
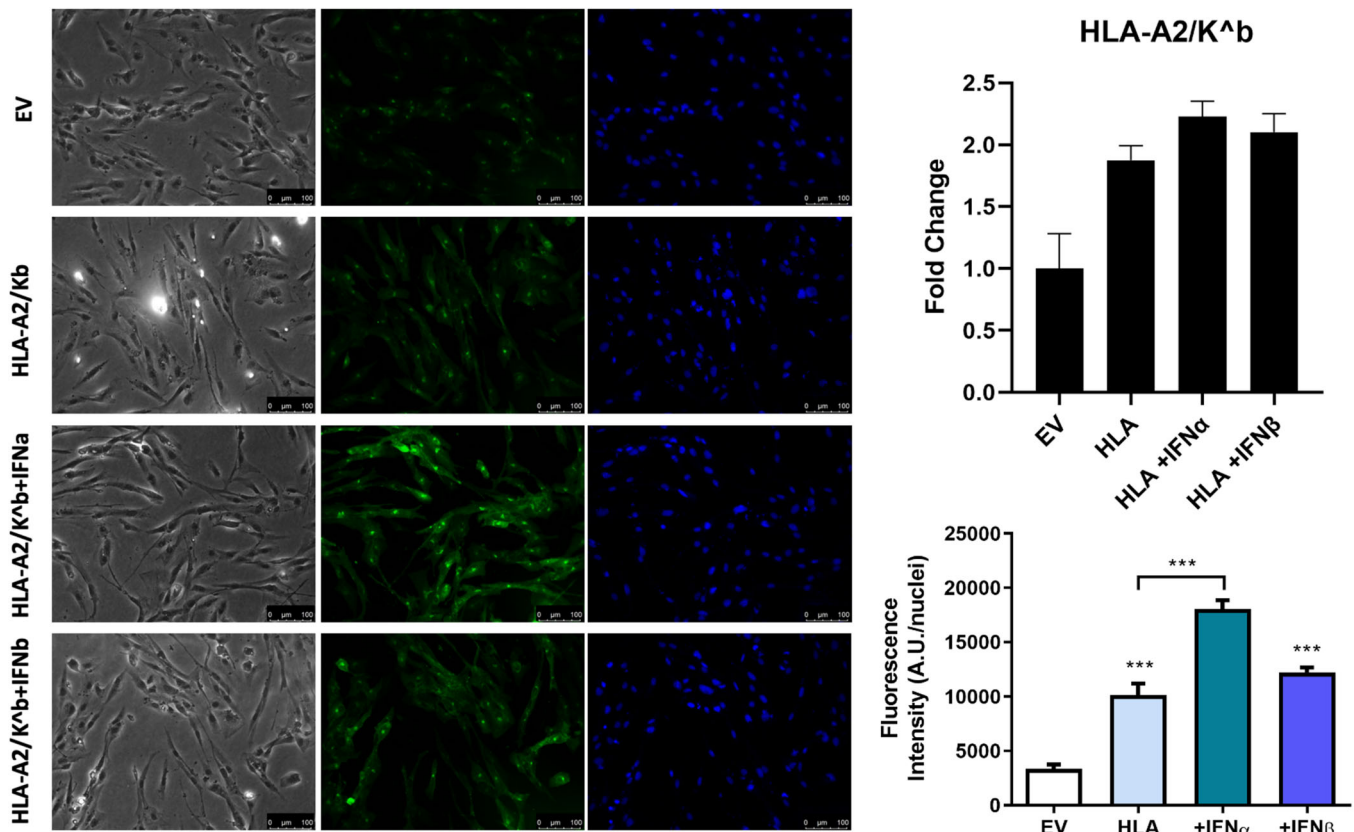
FIGURE 3 In-vitro overexpression of major histocompatibility complex-I. Representative phase contrast and single-channel fluorescent images of human skeletal muscle myoblasts transfected with human leukocyte antigen(HLA)-A2/K^b or empty vector (EV) in presence or absence of type I interferons stained with anti-HLA-I (green) and 4′,6′-diamidino-2-phenylindole dihydrochloride (blue). Images captured at 20× magnification. Scale bar = 100 μm. Quantification of HLA Class I fluorescence intensity level normalized to nuclei number. (c) HLA Class I gene expression. Data represent mean ± SEM, *$p \le 0.05$, ***$p < 0.001$ compared to EV or to HLA I-overexpressing cells. SEM, standard error of the mean.

3.6 | MHC-I overexpression in human myoblasts does not induce gross changes in mitochondrial structure or markers of mitochondrial dynamics

We examined mitochondrial structure in MHC-I overexpressing human myoblasts in the absence or presence of type I IFNs. There was no significant change in mitochondrial footprint, branch number or number of reticular branches (Figure 7). Moreover, there were no significant changes in the mitochondria dynamics markers, PPARG-C1A, MFN1, MFN2, OPA1, TFAM or Fis1 (Figure 8).

4 | DISCUSSION

Previous research has shown that MHC-I overexpression can induce ER stress, potentially driving skeletal muscle weakness in myositis in the absence of inflammatory infiltrates in muscle fibers (Englund et al., 2001; Li et al., 2009). Distinct IFN signatures have been suggested to act as biomarkers of different IIMs, with type I IFNs being predominantly seen in dermatomyositis and to a lesser degree in polymyositis (Greenberg, 2010). Given the bidirectional crosstalk

between ER and mitochondria, as well as evidence of mitochondrial abnormalities in the muscle of myositis patients (Alhatou et al., 2004; Boehler et al., 2019; Meyer et al., 2017; Thoma et al., 2020), this study aimed to assess the effects of MHC-I overexpression in human skeletal muscle myoblasts in the presence or absence of type I IFNs on mitochondrial functionality. The major findings of this research are that the negative impact of MHC-I overexpression on mitochondrial function membrane potential and aggravated by the presence of type IFNs, alongside a differential impact on RONS generation.

In this study, we observed that IFNα induced a further over-expression of MHC-I in the HLA-transfected human skeletal muscle model. This finding is consistent with previous studies showing IFNα induced long-lasting MHC-I overexpression in human beta cells (Coomans de Brachène et al., 2018; Marroqui et al. 2017). Moreover, a study in human primary skeletal muscle cells found that upregulated levels of HLA-ABC-induced type I IFN pathway activation, which inhibited myoblast differentiation and induced myotube atrophy in the context of diabetes (Ladislau et al., 2018). Here, we were able to reveal that it is IFNα, rather than IFNβ, that induced enhanced HLA-I expression in MHC-I overexpressing cells, highlighting the differential effects of IFNα and IFNβ on MHC class I regulation in human skeletal myoblasts.
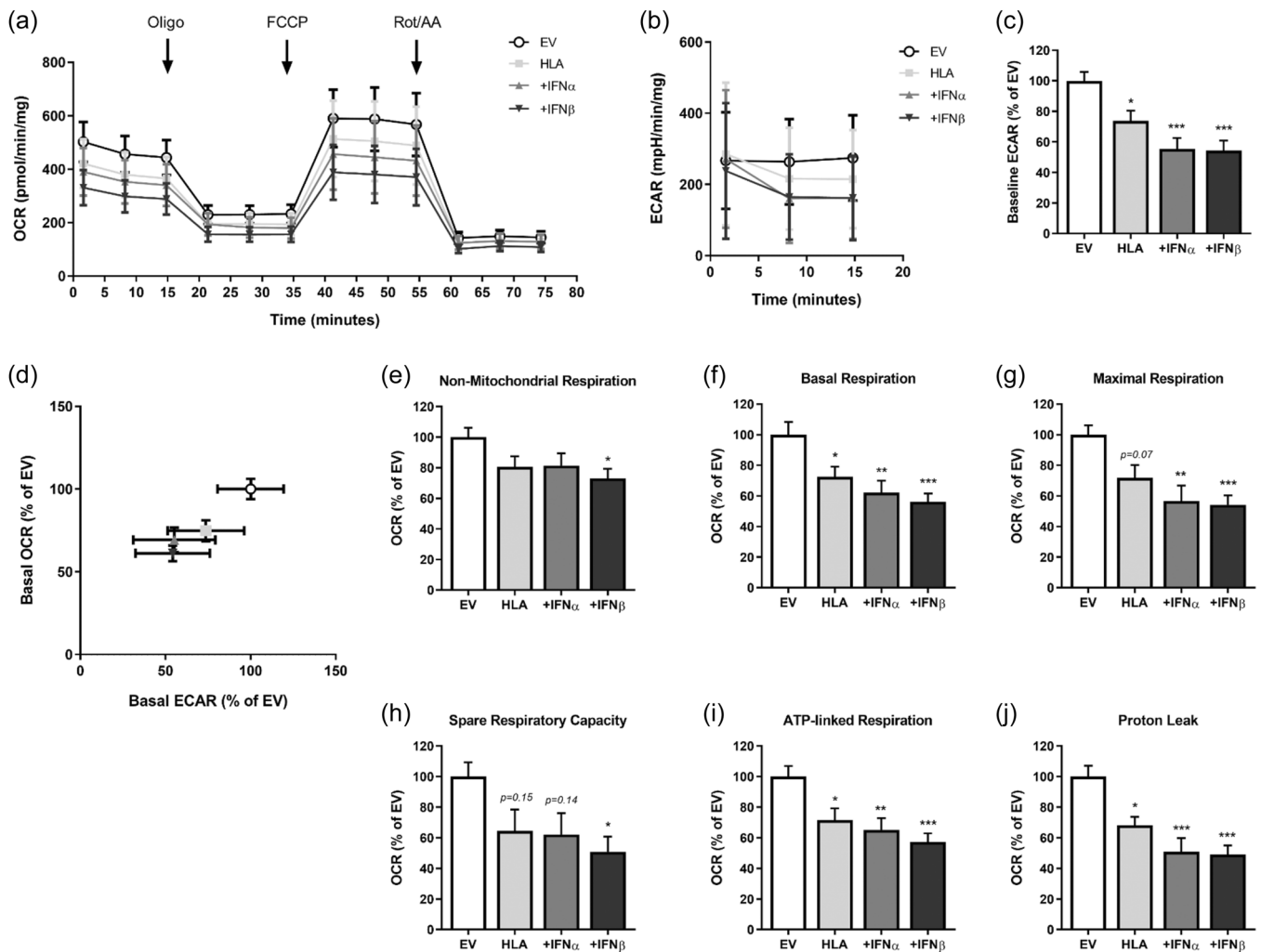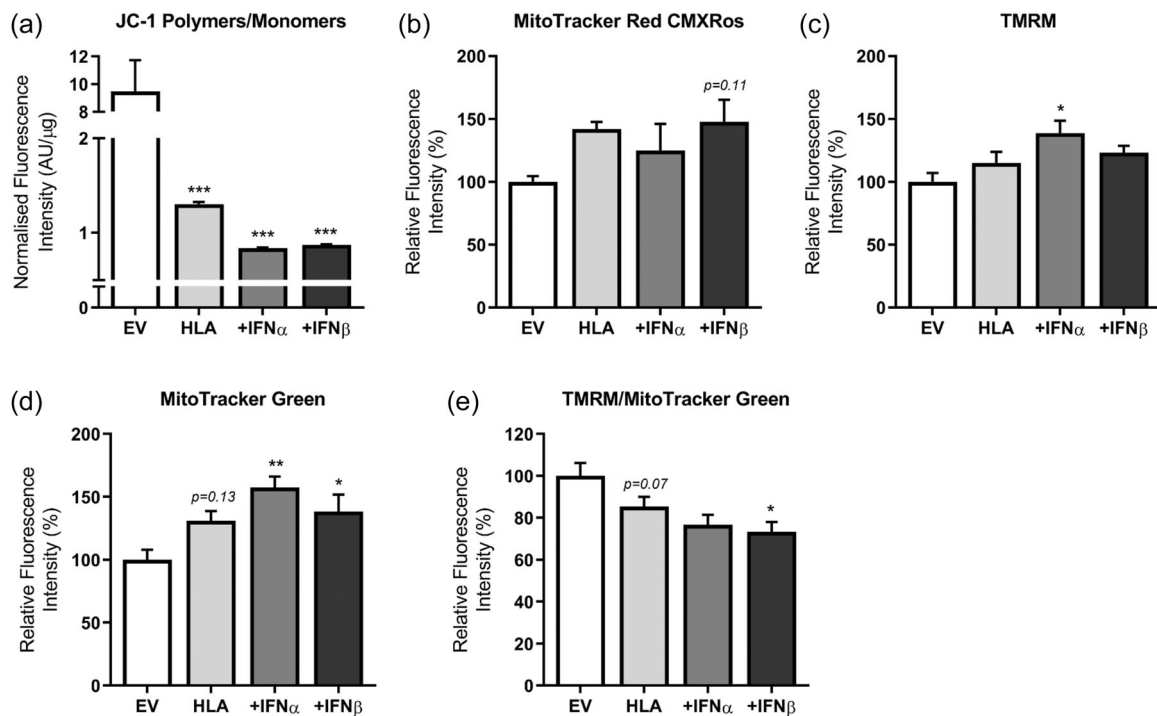
FIGURE 4 Mitochondrial function of human leukocyte antigen-I-transfected human myoblasts treated with or without type I interferons. (a) Real-time measurements of oxygen consumption rate (OCR) following the sequential injection of oligomycin, FCCP, and a mixture of rotenone/antimycin A. (b) Real-time measurements of extracellular acidification rate (ECAR) and (c) baseline ECAR values. (d) Bioenergetic profile expressed as OCR versus ECAR measured under basal condition. (e–j) Mitochondrial function parameters; nonmitochondrial respiration, basal respiration, maximal respiration, spare respiratory capacity, ATP-linked respiration, and proton leak, normalized to protein content ($n = 8$ per group). Data represent mean ± SEM, *$p \leq 0.05$, **$p < 0.01$, ***$p < 0.001$ compared to empty vector. ATP, adenosine triphosphate; FCCP, carbonyl cyanide-p-trifluoromethoxyphenylhydrazone; SEM, standard error of the mean.

While IFNα enhanced the expression of MHC-I, IFNβ induced stronger defects on mitochondrial function compared to IFNα, independent of MHC-I overexpression. More specifically, IFNα induced mild mitochondrial respiratory defects, specifically seen in basal and ATP-linked respiration, that only became evident after 24 h incubation at a concentration of 200 ng/mL, while such effects were already evident after 18 h incubation in the presence of 100 ng/mL IFNβ. This is consistent with IFNβ-induced mitochondrial damage reported in previous studies of brown adipose tissue (Kissig et al., 2017) and skeletal muscle (Meyer et al., 2017). However, the IFNβ-induced mitochondrial dysfunction can be considered moderate, as IFNβ seems to decrease basal, maximal, and ATP-linked respiration, but not reserve capacity, and such effects were returned to control values with longer exposure (24 h).

Our data show direct negative effects of MHC-I overexpression on mitochondrial respiration, as well as basal glycolysis, in human skeletal muscle cells. Interestingly, these effects were exacerbated in presence of type I IFNs. Mitochondrial impairments were also evident as mitochondrial membrane depolarization in response to MHC-I overexpression in combination with type I IFNβ. Further, a combinational effect of MHC-I overexpression and IFNβ increased mitochondrial mass, which may be interpreted as an attempt by the cells to compensate for respiratory deficits. Interestingly, Kissig et al. (2017) reported in brown adipocytes no IFNα-induced changes increase in mitochondrial biogenesis (Kissig et al., 2017), but IFNβ was not studied. This is further supported by our immunofluorescent imaging, revealing an increased mitochondrial footprint in MHC I overexpressing cells, which was enhanced in the presence of type I IFNs.

FIGURE 5 Mitochondrial mass and membrane potential of human leukocyte antigen-I-transfected human myoblasts treated with or without type I interferons. (a) Mitochondrial membrane potential expressed as JC-1 aggregates (red fluorescence) to JC-1 monomers (green fluorescence) ratio normalized to protein content ($n = 6$). (b–d) Fluorescence intensity changes of MitoTracker Red CMXRos and tetramethylrhodamine (TMRM) indicative of changes in mitochondrial membrane potential of active mitochondria only, as well as of MitoTracker Green, representing changes in mitochondrial mass. (e) Fluorescence intensity of TMRM normalized to MitoTracker Green. Data represent mean ± SEM, $*p \leq 0.05$, $**p < 0.01$, $***p < 0.001$ compared to empty vector. SEM, standard error of the mean.
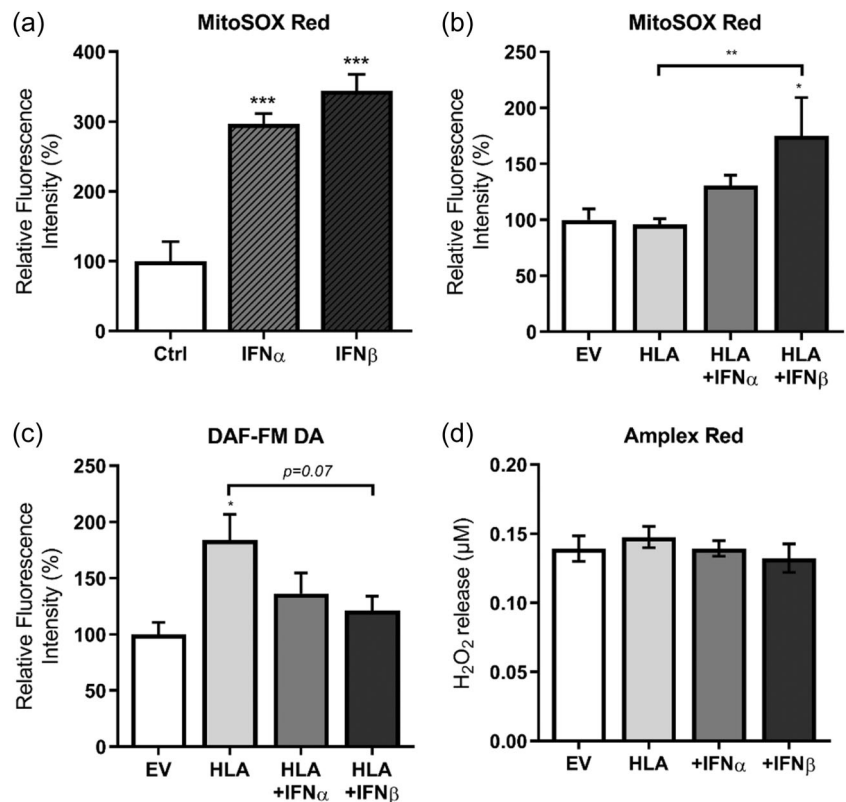
FIGURE 6 RONS generation in human leukocyte antigen (HLA)-I-transfected human myoblasts treated with or without type I interferons (IFNs). (a and b) Fluorescence intensity levels of MitoSOX Red, an indicator of mitochondrial superoxide generation, induced by type I IFNs or major histocompatibility complex-I overexpressing cells with or without type I IFNs ($n = 3$–8), and (c) DAF-FM DA, showing cellular nitric oxide generation ($n = 4$). (d) Release of hydrogen peroxide from cells as measured by Amplex Red assay. All data were normalized to protein content. Data represent mean ± SEM, $*p \leq 0.05$, $**p < 0.01$, $***p < 0.001$ compared to empty vector or HLA I-overexpressing cells. DAF-FM DA, 4-amino-5-methylamino-2',7'-difluorofluorescein diacetate; RONS, reactive oxygen & nitrogen species; SEM, standard error of the mean.
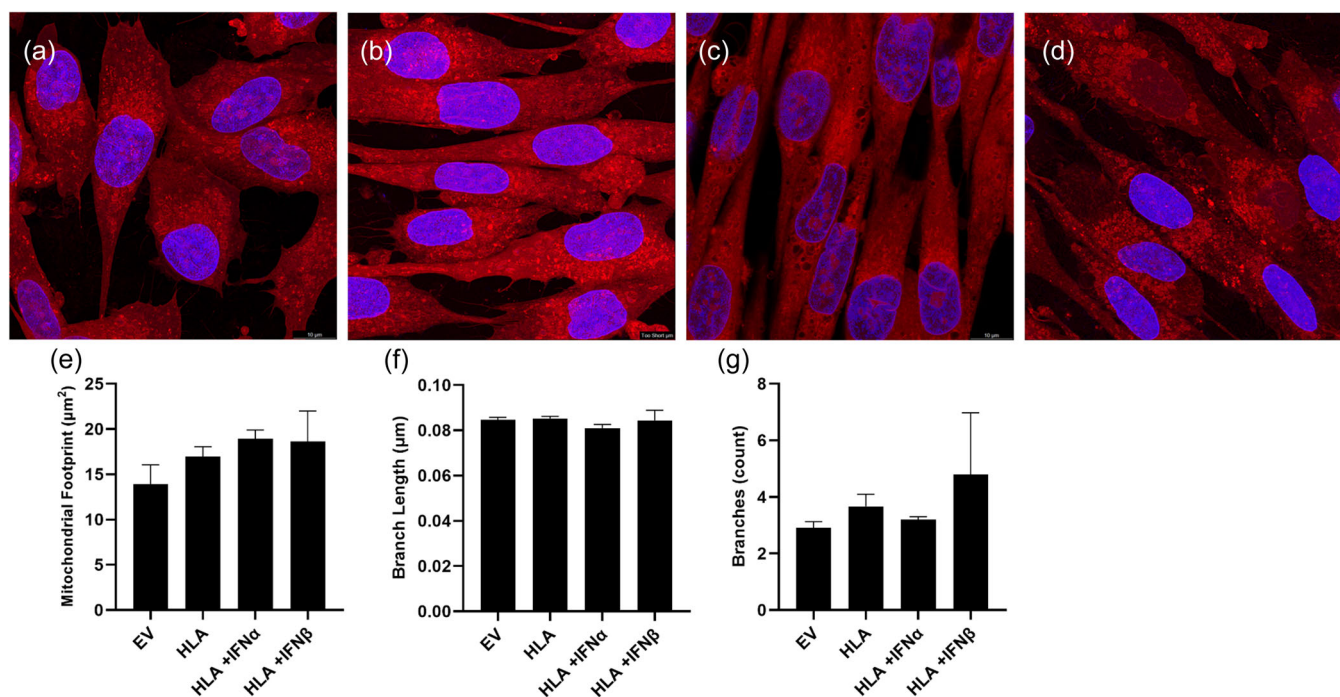
FIGURE 7 Immunofluorescent imaging of human skeletal muscle myoblasts transfected with empty vector (a) human leukocyte antigen-A2/K^b (b) in presence or absence of inteferon alpha (c) or interferon beta (d), with MitoTracker Red dye and 4′,6′-diamidino-2-phenylindole dihydrochloride, with quantification of reticular structure using mitochondrial network analysis. reporting mitochondrial footprint (e), branch length (f) and branch count (g). Data are presented as mean ± SEM, (n = 4).

Although we cannot draw a firm conclusion, the observed increase in mitochondrial mass in our study may be the result of a synergistic action of MHC-I overexpression and type I IFN. Further studies are warranted to examine the effects of individual type I IFNs in this matter. Altogether, these findings suggest that there is a synergistic impact of MHC-I overexpression and type I IFNs on mitochondrial biogenesis, function, and membrane polarization in human muscle myoblasts. Interestingly, we saw no clear changes in genes which regulate mitochondrial biogenesis, fusion or fission, across all experimental conditions. This could be attributed to the temporal nature of the treatments and the qPCR analyses.

Reactive oxygen and nitrogen species have been reported to play an important role in the pathogenesis of several myopathies other than myositis. Hence it is possible that reactive oxygen and nitrogen species are involved in myositis-associated muscle weakness (Lightfoot et al., 2015). Indeed, the involvement of nitric oxide in inflammatory myopathies has been reported by Tews and Goebel (1998), who showed inducible and neuronal nitric oxide synthase upregulation in the muscle fibers of 21 patients with myositis (Tews & Goebel, 1998). Another study has also shown elevated inducible nitric oxide synthase and nitric oxide levels, as assessed by nitrated tyrosine residue staining, in the muscle fibers of sporadic inclusion body myositis and to a lower degree in dermatomyositis (Schmidt et al., 2012). However, the role of reactive oxygen and nitrogen species in myositis are poorly understood. The present study showed that both IFNα and IFNβ contribute to mitochondrial ROS generation, as indicated by increases in mitochondrial superoxide levels,

while MHC-I overexpression alone showed no significant increase in mitochondrial superoxide generation. This observation is consistent with a previous study showing IFNβ-induced reactive oxygen species generation in a dose-dependent manner (Meyer et al., 2017). In our study, mitochondrial superoxide generation was also highly induced in MHC-I overexpressing myoblasts in the presence of type I IFNs, with IFNβ-treated MHC-I overexpressing cells showing statistically significant increase. It was surprising, however, that IFNα-treated MHC-I overexpressing cells showed no significant increase in mitochondrial superoxide generation, considering pronounced elevations observed by IFNα treatment alone. Surprisingly, IFNβ-treated MHC-I overexpressing cells showed a less robust increase in mitochondrial superoxide compared to IFNβ-treated cells only. One explanation for this unexpected observation is that previous studies have shown that nitric oxide can react with superoxide producing peroxynitrite, which may result in an overall decreased superoxide availability (Ott et al., 2007; Pearson et al., 2014) and the increased levels of nitric oxide during MHC-I overexpression may have scavenged the oxygen radicals that have been generated as a result of IFN. Alternatively, these data may suggest MHC I overexpression has a blunting effect on mitochondrial superoxide generation, when used in combination with type I IFNs. Moreover, we observed a decline in DAF-FM DA (marker of NO⁻ generation) fluorescence in the presence of IFNs, compared with MHC I overexpression alone. Thus, overall, these findings highlight a potential differential impact of MHC I overexpression and type I IFNs on ROS generation. Further investigations of ROS generation in our study showed no changes in the release of
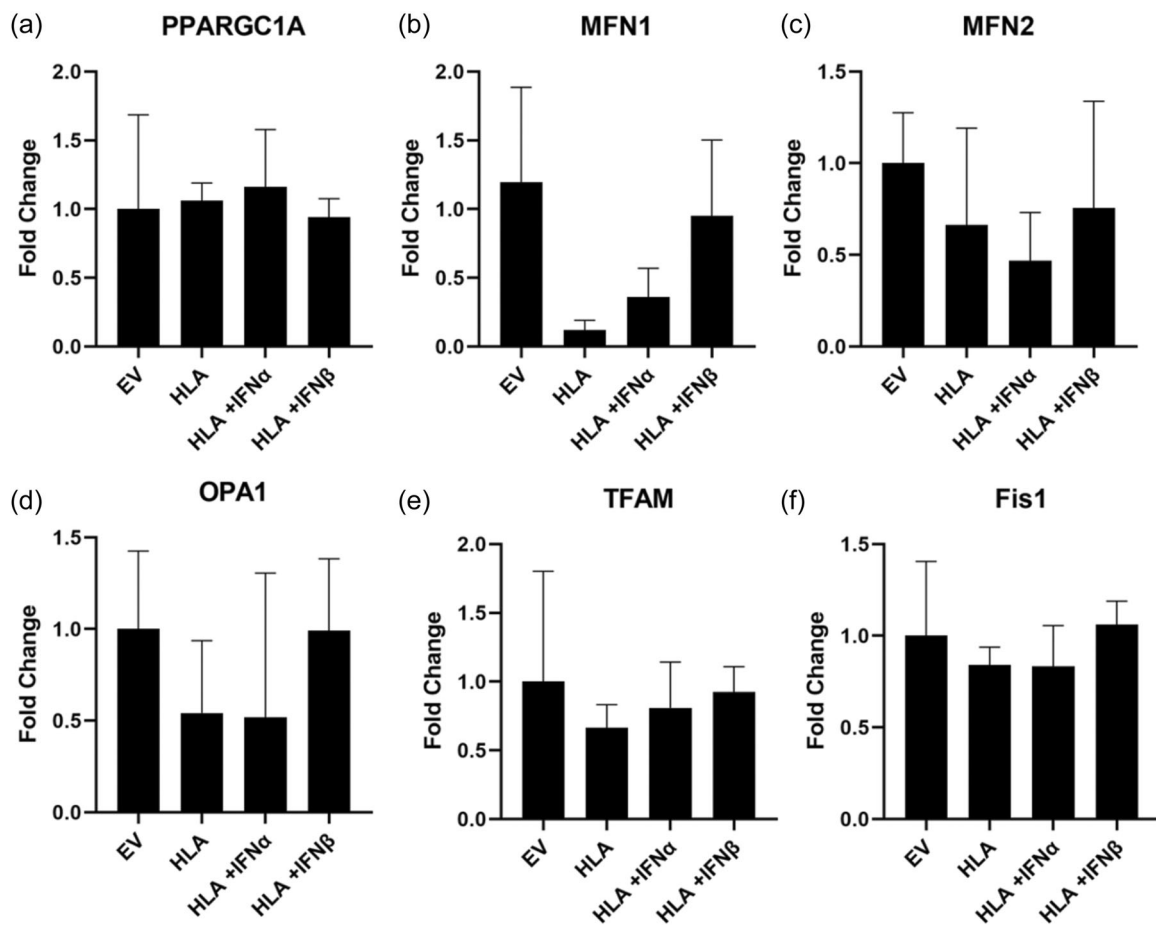
FIGURE 8 Quantitative polymerase chain reaction data showing changes in gene expression of PPARGC1 (a), MFN1 (b), MFN2 (c), OPA1 (d), TFAM (e) and Fis1 (f), expressed as fold change, in human skeletal muscle myoblasts transfected with human leukocyte antigen-A2/K^b or empty vector in presence or absence of type I interferons. Data are presented as mean ± SEM, (n = 4). SEM, standard error of the mean.

hydrogen peroxide in MHC-I overexpressing cells in presence or absence of type I IFNs. In further support of these findings, both IFNα and IFNβ showed inhibitory effects on nitric oxide production in endothelial cells (Buie et al., 2017; Jia et al., 2018).

There are limitations to the present study, mechanistically type I IFNs are well characterized activators or both the JAK-STAT and NF-kB pathway (Majoros et al., 2017; Pfeffer, 2011; Rubio et al., 2013). We do not present evidence to support either, however, further investigation is needed using gene knockdown technologies, to provide further insight, as these pathways can be targeted therapeutically by a range of pharmacological compounds. Animal preclinical models of myositis may have some utility in assessing the applicability of our findings to human disease (Nagaraju et al., 2000). However, we reason that animals are a poor surrogate for human physiology overall, (Marshall et al., 2023).

Further, as our findings are obtained in a human muscle cell model of myositis and need to be verified in human patient cells. Thus, although MHC-I overexpression is a key hallmark of myositis, the magnitude of overexpression in our model may not be representative of the levels of MHC I expressed on the surface of a patient's muscle cells. Similarly, the levels of IFNs we utilized in vitro may not reflect the levels seen in muscles from patients.

The present findings provide novel insights into the differential effects of two major type I IFNs, namely IFNα and IFNβ, on mitochondrial respiration, membrane polarization and a differential impact on RONS generation. This study also shows the effects of MHC-I overexpression and type I IFNs specifically on mitochondrial function, acting synergistically in inducing respiratory defects and a loss of mitochondrial membrane potential. Moreover, it is of great interest that MHC-I overexpression and type I IFNs exert distinct effects on reactive oxygen and nitrogen species production, with MHC-I overexpression contributing to nitric oxide generation but type I IFNs alleviating this effect, and IFNs promoting mitochondrial superoxide production. Hence, these findings have important implications in myositis pathogenesis and warrant further investigation.

AUTHOR CONTRIBUTIONS

CONFLICT OF INTEREST STATEMENT

The authors declare no conflict of interest.

DATA AVAILABILITY STATEMENT

The data that support the findings of this study are available from the corresponding author upon reasonable request.

ORCID

Nasser Al-Shanti http://orcid.org/0000-0002-4215-2649
Adam P. Lightfoot http://orcid.org/0000-0003-1501-7879

REFERENCES

Alhatou, M. I., Sladky, J. T., Bagasra, O., & Glass, J. D. (2004). Mitochondrial abnormalities in dermatomyositis: Characteristic pattern of neuropathology. *Journal of Molecular Histology*, 35(6), 615–619.

Arshanapalli, A., Shah, M., Veerula, V., & Somani, A. K. (2015). The role of type I interferons and other cytokines in dermatomyositis. *Cytokine*, 73(2), 319–325.

Boehler, J. F., Horn, A., Novak, J. S., Li, N., Ghimbovschi, S., Lundberg, I. E., Alexanderson, H., Alemo Munters, L., Jaiswal, J. K., & Nagaraju, K. (2019). Mitochondrial dysfunction and role of harakiri in the pathogenesis of myositis. *The Journal of Pathology*, 249(2), 215–226.

Buie, J. J., Renaud, L. L., Muise-Helmericks, R., & Oates, J. C. (2017). IFN-α negatively regulates the expression of endothelial nitric oxide synthase and nitric oxide production: Implications for systemic lupus erythematosus. *The Journal of Immunology*, 199(6), 1979–1988.

Carstens, P. O., & Schmidt, J. (2014). Diagnosis, pathogenesis and treatment of myositis: Recent advances. *Clinical and Experimental Immunology*, 175(3), 349–358.

Coomans de Brachène, A., Dos Santos, R. S., Marroqui, L., Colli, M. L., Marselli, L., Mirmira, R. G., Marchetti, P., & Eizirik, D. L. (2018). IFN-α induces a preferential long-lasting expression of MHC class I in human pancreatic beta cells. *Diabetologia*, 61(3), 636–640.

Cruz-Tapias, P., Castiblanco, J., & Anaya, J. M. (2013). Major histocompatibility complex: Antigen processing and presentation, In J. M. Anaya, Y. Shoenfeld, A. Rojas-Villarraga, R. A. Levy, & R. Cervera (Eds.), *Autoimmunity: From bench to bedside [Internet]*. El Rosario University Press.

Danieli, M. G., Antonelli, E., Piga, M. A., Cozzi, M. F., Allegra, A., & Gangemi, S. (2023). Oxidative stress, mitochondrial dysfunction, and respiratory chain enzyme defects in inflammatory myopathies. *Autoimmunity Reviews*, 22(5), 103308.

Dott, W., Mistry, P., Wright, J., Cain, K., & Herbert, K. E. (2014). Modulation of mitochondrial bioenergetics in a skeletal muscle cell line model of mitochondrial toxicity. *Redox Biology*, 2, 224–233.

Englund, P., Lindroos, E., Nennesmo, I., Klareskog, L., & Lundberg, I. E. (2001). Skeletal muscle fibers express major histocompatibility complex class II antigens independently of inflammatory infiltrates in inflammatory myopathies. *The American Journal of Pathology*, 159(4), 1263–1273.

Fréret, M., Drouot, L., Obry, A., Ahmed-Lacheheb, S., Dauly, C., Adriouch, S., Cosette, P., Authier, F. J., & Boyer, O. (2013). Overexpression of MHC class I in muscle of lymphocyte-deficient mice causes a severe myopathy with induction of the unfolded protein response. *The American Journal of Pathology*, 183(3), 893–904.

Greenberg, S. A. (2010). Type 1 interferons and myositis. *Arthritis Research & Therapy*, 12(1), 1–7.

Irwin, M. J., Heath, W. R., & Sherman, L. A. (1989). Species-restricted interactions between CD8 and the alpha 3 domain of class I influence the magnitude of the xenogeneic response. *The Journal of Experimental Medicine*, 170(4), 1091–1101.

Jia, H., Thelwell, C., Dilger, P., Bird, C., Daniels, S., & Wadhwa, M. (2018). Endothelial cell functions impaired by interferon in vitro: Insights into the molecular mechanism of thrombotic microangiopathy associated with interferon therapy. *Thrombosis Research*, 163, 105–116.

Kissig, M., Ishibashi, J., Harms, M. J., Lim, H. W., Stine, R. R., Won, K. J., & Seale, P. (2017). PRDM16 represses the type I interferon response in adipocytes to promote mitochondrial and thermogenic programing. *The EMBO Journal*, 36(11), 1528–1542.

Ladislau, L., Suárez-Calvet, X., Toquet, S., Landon-Cardinal, O., Amelin, D., Depp, M., Rodero, M. P., Hathazi, D., Duffy, D., Bondet, V., Preusse, C., Bienvenu, B., Rozenberg, F., Roos, A., Benjamim, C. F., Gallardo, E., Illa, I., Mouly, V., Stenzel, W., ... Allenbach, Y. (2018). JAK inhibitor improves type I interferon induced damage: Proof of concept in dermatomyositis. *Brain*, 141(6), 1609–1621.

Li, C. K., Knopp, P., Moncrieffe, H., Singh, B., Shah, S., Nagaraju, K., Varsani, H., Gao, B., & Wedderburn, L. R. (2009). Overexpression of MHC class I heavy chain protein in young skeletal muscle leads to severe myositis. *The American Journal of Pathology*, 175(3), 1030–1040.

Lightfoot, A. P., McArdle, A., Jackson, M. J., & Cooper, R. G. (2015). In the idiopathic inflammatory myopathies (IIM), do reactive oxygen species (ROS) contribute to muscle weakness? *Annals of the Rheumatic Diseases*, 74(7), 1340–1346.

Majoros, A., Platanitis, E., Kernbauer-Hölzl, E., Rosebrock, F., Müller, M., & Decker, T. (2017). Canonical and non-canonical aspects of JAK–STAT signaling: Lessons from interferons for cytokine responses. *Frontiers in Immunology*, 8, 29.

Mamchaoui, K., Trollet, C., Bigot, A., Negroni, E., Chaouch, S., Wolff, A., Kandalla, P. K., Marie, S., Di Santo, J., St Guily, J. L., Muntoni, F., Kim, J., Philippi, S., Spuler, S., Levy, N., Blumen, S. C., Voit, T., Wright, W. E., Aamiri, A., ... Mouly, V. (2011). Immortalized pathological human myoblasts: Towards a universal tool for the study of neuromuscular disorders. *Skeletal Muscle*, 1(1), 34.

Marroqui, L., Dos Santos, R. S., Op de beeck, A., Coomans de Brachène, A., Marselli, L., Marchetti, P., & Eizirik, D. L. (2017). Interferon-α mediates human beta cell HLA class I overexpression, endoplasmic reticulum stress and apoptosis, three hallmarks of early human type 1 diabetes. *Diabetologia*, 60(4), 656–667.

Marshall, L. J., Bailey, J., Cassotta, M., Herrmann, K., & Pistollato, F. (2023). Poor translatability of biomedical research using animals—A narrative review. *Alternatives to Laboratory Animals*, 51(2), 102–135.

Meyer, A., Laverny, G., Allenbach, Y., Grelet, E., Ueberschlag, V., Echaniz-Laguna, A., Lannes, B., Alsaleh, G., Charles, A. L., Singh, F., Zoll, J., Lonsdorfer, E., Maurier, F., Boyer, O., Gottenberg, J. E., Nicot, A. S., Laporte, J., Benveniste, O., Metzger, D., ... Geny, B. (2017). IFN-β-induced reactive oxygen species and mitochondrial damage contribute to muscle impairment and inflammation maintenance in dermatomyositis. *Acta Neuropathologica*, 134(4), 655–666.

Nagaraju, K., Casciola-Rosen, L., Lundberg, I., Rawat, R., Cutting, S., Thapliyal, R., Chang, J., Dwivedi, S., Mitsak, M., Chen, Y. W., Plotz, P., Rosen, A., Hoffman, E., & Raben, N. (2005). Activation of the endoplasmic reticulum stress response in autoimmune myositis: Potential role in muscle fiber damage and dysfunction. *Arthritis and Rheumatism*, *52*(6), 1824–1835.

Nagaraju, K., Raben, N., Loeffler, L., Parker, T., Rochon, P. J., Lee, E., Danning, C., Wada, R., Thompson, C., Bahtiyar, G., Craft, J., Hooft van Huijsduijnen, R., & Plotz, P. (2000). Conditional upregulation of MHC class I in skeletal muscle leads to self-sustaining autoimmune myositis and myositis-specific autoantibodies. *Proceedings of the National Academy of Sciences*, *97*(16), 9209–9214.

Ott, M., Gogvadze, V., Orrenius, S., & Zhivotovsky, B. (2007). Mitochondria, oxidative stress and cell death. *Apoptosis*, *12*(5), 913–922.

Pearson, T., Kabayo, T., Ng, R., Chamberlain, J., McArdle, A., & Jackson, M. J. (2014). Skeletal muscle contractions induce acute changes in cytosolic superoxide, but slower responses in mitochondrial superoxide and cellular hydrogen peroxide. *PLoS One*, *9*(5), e96378.

Pfeffer, L. M. (2011). The role of nuclear factor κB in the interferon response. *Journal of Interferon & Cytokine Research*, *31*(7), 553–559.

Rigolet, M., Hou, C., Baba Amer, Y., Aouizerate, J., Periou, B., Gherardi, R. K., Lafuste, P., & Authier, F. J. (2019). Distinct interferon signatures stratify inflammatory and dysimmune myopathies. *RMD Open*, *5*(1), e000811.

Rubio, D., Xu, R. H., Remakus, S., Krouse, T. E., Truckenmiller, M. E., Thapa, R. J., Balachandran, S., Alcamí, A., Norbury, C. C., & Sigal, L. J. (2013). Crosstalk between the type 1 interferon and nuclear factor kappa B pathways confers resistance to a lethal virus infection. *Cell Host & Microbe*, *13*(6), 701–710.

Schmidt, J., Barthel, K., Zschüntzsch, J., Muth, I. E., Swindle, E. J., Hombach, A., Sehmisch, S., Wrede, A., Lühder, F., Gold, R., & Dalakas, M. C. (2012). Nitric oxide stress in sporadic inclusion body myositis muscle fibres: Inhibition of inducible nitric oxide synthase prevents interleukin-1β-induced accumulation of β-amyloid and cell death. *Brain*, *135*(4), 1102–1114.

Sivandzade, F., Bhalerao, A., & Cucullo, L. (2019). Analysis of the mitochondrial membrane potential using the cationic JC-1 dye as a sensitive fluorescent probe. *Bio-protocol*, *9*(1), e3128.

Tews, D. S., & Goebel, H. H. (1998). Cell death and oxidative damage in inflammatory myopathies. *Clinical Immunology and Immunopathology*, *87*(3), 240–247.

Thoma, A., Earl, K. E., Goljanek-Whysall, K., & Lightfoot, A. P. (2022). Major histocompatibility complex I-induced endoplasmic reticulum stress mediates the secretion of pro-inflammatory muscle-derived cytokines. *Journal of Cellular and Molecular Medicine*, *26*(24), 6032–6041.

Thoma, A., Lyon, M., Al-Shanti, N., Nye, G. A., Cooper, R. G., & Lightfoot, A. P. (2020). Eukarion-134 attenuates endoplasmic reticulum stress-induced mitochondrial dysfunction in human skeletal muscle cells. *Antioxidants*, *9*(8), 710.

Valente, A. J., Maddalena, L. A., Robb, E. L., Moradi, F., & Stuart, J. A. (2017). A simple ImageJ macro tool for analyzing mitochondrial network morphology in mammalian cell culture. *Acta Histochemica*, *119*(3), 315–326.

Walsh, R. J., Kong, S. W., Yao, Y., Jallal, B., Kiener, P. A., Pinkus, J. L., Beggs, A. H., Amato, A. A., & Greenberg, S. A. (2007). Type I interferon–inducible gene expression in blood is present and reflects disease activity in dermatomyositis and polymyositis. *Arthritis and Rheumatism*, *56*(11), 3784–3792.